J. Membrane Biol. 185, 83–92 (2002)
DOI: 10.1007/s00232-001-0113-2

The Journal of
Membrane
Biology

Electrophysiological Behavior of the TolC Channel-Tunnel in Planar Lipid Bilayers

C. Andersen, C. Hughes, V. Koronakis
Cambridge University Department of Pathology, Tennis Court Road, Cambridge CB2 1QP, UK

Received: 23 May 2001/Revised: 14 August 2001

Abstract. *Escherichia coli* TolC assembles into the unique channel-tunnel structure spanning the outer membrane and periplasmic space. The structure is constricted only at the periplasmic entrance of the tunnel and this must be opened to allow export of substrates bound by cognate inner membrane complexes. We have investigated the electrophysiological behavior of TolC reconstituted into planar lipid bilayers, in particular the influence of the membrane potential, the electrolyte concentration and pH. TolC inserted in one orientation into the membrane. The resultant pores were stable and showed no voltage-dependent opening or closing. Nevertheless, TolC could adopt up to three conductance substates. The pores were cation-selective with a permeability ratio of potassium to chloride ions of 16.5. The single-channel conductance was higher when the protein was inserted from the side with negative potential. It showed a nonlinear dependence on the concentration of the electrolyte in the bulk solution and decreased as the pH was lowered. The calculated pK of the apparent closing was 4.5. The electrophysiological characterization is discussed in relation to the TolC structure, in particular the periplasmic entrance.

Key words: TolC — Electrophysiology — Channel-tunnel — Type I secretion — Multidrug efflux pump

Introduction

TolC is a trimeric outer membrane protein of *Escherichia coli*. It is central to the type I export of large protein toxins (Koronakis, Koronakis & Stauffer, 1997; Wandersman & Delepelaire, 1990) and to multidrug efflux (Fralick, 1996; Zgurskaya & Nikaido, 2000). During export, it is recruited by specific substrate-bound, energized complexes in the cytoplasmic membrane. In this way, substrates bypass the periplasm and exit the cell (Koronakis et al., 1997; Thanabalu et al., 1998). TolC is anchored in the outer membrane by a 40-Å long β-barrel (the channel domain) and spans the periplasmic space via a contiguous 100-Å long α-helical barrel (the tunnel domain). The assembled channel-tunnel forms a single pore with a diameter of 35 Å, providing a 43,000 $Å^3$ water-filled exit duct (Koronakis et al., 2000). While the TolC outer membrane channel is constitutively open to the cell exterior, towards the tunnel periplasmic entrance the inner diameter decreases to a virtual close to provide the only constriction of the structure. The entrance must therefore be opened and it is envisaged that the substrate-dependent recruitment of TolC triggers an iris-like opening involving movement of the three pairs of α-helices that form the aperture (Koronakis et al., 2000). The principal structural elements of TolC are conserved throughout a large family of homologues, suggesting that this is a common mechanism underlying export and efflux events throughout Gram-negative bacteria (Koronakis et al., 2000; Andersen, Hughes & Koronakis, 2000).

Channel-tunnel behavior can now be investigated in the context of the structure, which is distinct from other outer membrane proteins (Cowan et al., 1992; Forst et al., 1998; Andersen et al., 2000). This study presents an electrophysiological characterization of purified TolC reconstituted into lipid bilayers. While some of the experimental conditions applied are unphysiological, they facilitate understanding of the electrophysiological behaviour of this protein and establish a basis for a study of the TolC structure function relationship.

Correspondence to: V. Koronakis; email: vk103@mole.bio.cam.ac.uk

Materials and Methods

TolC Protein Purification

TolC protein was expressed and purified after isopropyl β-D-thio-galactopyranoside (IPTG)-induction of *E. coli* BL21 (DE3) carrying the recombinant plasmid pT7TolC (Koronakis et al., 2000). Cells were broken in a French press, the membranes collected (50,000 × g, 40 min) and washed twice in 20 mM Tris HCl, pH 7.4, 20 mM $MgCl_2$, 0.5% Triton X-100 (Bio-Rad). TolC was solubilized from the membrane in 20 mM Tris- HC1, pH 7.4, 20 mM $MgCl_2$, 5% Triton X-100, 10% glycerol, and insoluble material removed (50,000 × g, 20 min). TolC was then purified from the supernatant by binding on a Q sepharose anion exchange column (5ml Hitrap Q, Pharmacia) and elution with a NaCl gradient in 20 mM Tris, pH 7.4, 0.5% Triton X-100. The TolC was pure as analyzed by SDS-PAGE.

Conductance Measurements

Instrumentation comprised a Teflon chamber with two aqueous compartments connected by a small circular hole (diameter 0.5 mm). Black lipid membranes were formed as described previously (Benz et al., 1978), by painting onto the hole a 1% solution of diphytanoyl phosphatidylcholin (Avanti Polar Lipids, Alabaster, AL) in *n*-decane. The aqueous KCl solutions (Aldrich) were buffered by HEPES and citrate (Sigma, Poole, Dorset, UK). The temperature was kept at 20°C throughout. TolC was diluted in 0.5% Triton and was added to one side of the membrane (there were no differences when protein was added to the front or the back compartment of the apparatus, excluding asymmetries in the experimental setup). The membrane current was measured with a pair of calomel electrodes connected in series to a voltage source and an electrometer (Keithley 6517A, Reading, UK). The resistance of each membrane under the specific conditions was tested before adding TolC to the aqueous solution. Only membranes with resistance higher than 200 GΩ measured at a potential of 120 mV were used to perform the experiments. Control experiments confirmed that neither electrolyte concentration, pH, nor high potential as used in our measurements had an effect on the membranes. For single-channel recordings the electrometer was replaced by a current amplifier (Keithley 428). The amplified, filtered signal (Filter rise time 30 msec) was monitored using a strip chart-recorder. It was recorded with a sampling rate of 50 sec^{-1} by a PC connected to the output signal by an A/D-converting card (Keithley DAS-1601).

Selectivity Measurements

For the zero-current membrane potentials the membranes were formed in a 30 mM KCl solution (l mM HEPES, 7.5). TolC was added to either side of the membrane and the increase of the membrane conductance due to insertion of pores was observed with the electrometer. When a conductance of at least 2 nS was reached, corresponding to at least 100 inserted TolC channels (the single-channel conductance of TolC in 30 mM KCl is around 20 pS), the instrumentation was switched to the measurement of the zero-current potential and the KCl gradient was established by adding 3 M KCl solution to one side of the membrane while stirring. The zero-current membrane voltage reached its final value after 2–5 min. Single-channel experiments were used throughout to provide information on the changes in conductivity, noise and substate-switching frequency, but the results were confirmed in specific multichannel experiments.

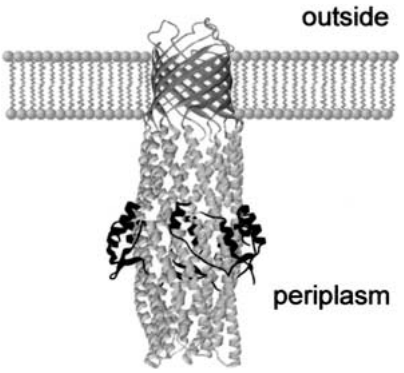

Fig. 1. Structure of the TolC channel-tunnel. The 40-Å long channel domain (grey) is assembled by 12 β-sheets (4 per monomer) and spans the outer membrane. The 100-Å long tunnel domain (light grey) projects into the periplasmic space. It is formed by four α-helical strands per monomer (two continous long helices and two pairs of shorter helices). A third domain, a mixed α/β-structure (black) forms a strap around the equator of the tunnel. The decreased inner diameter of the channel-tunnel at the periplasmic entrance provides the only constriction.

Results

Influence of the Membrane Potential on TolC Conductance

The TolC structure is highly asymmetric (Fig. 1), dictating channel insertion into the bacterial outer membrane with the tunnel domain projecting into the periplasmic space. We first assessed the dependence of the single-channel conductance of membrane-inserted TolC on the polarity of the applied potential. TolC was added to one side of black lipid membranes. Throughout, this side is referred to as the TolC-proximal side, and the potential is always given with respect to this side. The conductance was measured at either +80 mV (Fig. 2 upper trace) or −80 mV (Fig. 2 lower trace). After addition of TolC protein, conductance increased step-wise as single TolC molecules inserted into the artificial bilayer. Analysis of at least 100 single insertion events showed that the polarity of the membrane potential affected the conductance of TolC. The mean conductance was 81.5 ± 1.0 pS when the potential was positive, and 89.2 ± 1.7 pS when it was negative. It was evident that TolC can adopt or 'switch into' more than one conductance substate (Fig. 2 inset). When the potential was positive, insertion did not increase the noise (when compared to the zero line), but when the potential was negative the noise increased with each newly inserted TolC.

To confirm that the polarity-dependent behavior was an intrinsic property of membrane-inserted TolC, we assayed the influence of membrane potential in a single-channel experiment. In this case, only

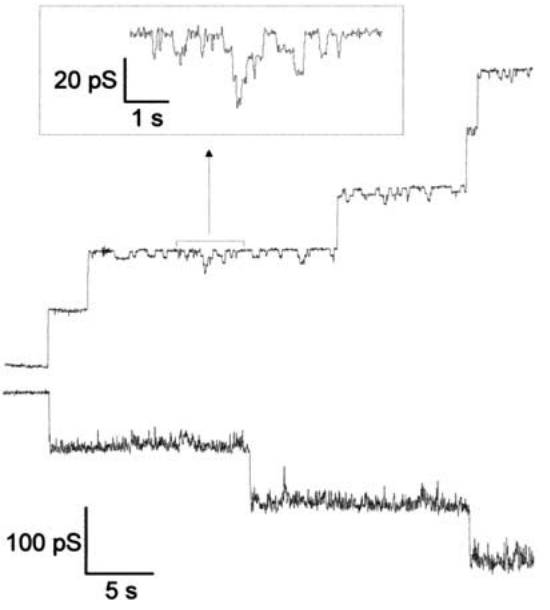

Fig. 2. Single-channel conductance of TolC measured at membrane potentials of +80 mV (upper trace) and −80 mV (lower trace). The membrane was formed by diphytanoyl-phosphatidylcholine/*n*-decane. TolC protein was added (final concentration of 10 pg/ml) to 1 M KCl, pH 7.5 electrolyte solution. The inset shows a higher amplitude resolution of the indicated trace.

very small amounts of protein (final concentration 1–5 pg/ml) were added to one side of the membrane so that a single conductance step was observed only after 10–60 min. The current through TolC increased with increasing voltage (Fig. 3*A*), and the conductance remained stable even at high voltages (±120 mV), indicating that no voltage-dependent closing or opening occurred. In Fig. 3*B* the traces for +100 mV, +40 mV, −40 mV and −100 mV are shown at higher resolution, illustrating more clearly the substates, even at negative potentials. The trace of +100 mV shows that a single TolC can switch into three distinct substates (*S1*, *S2*, *S3*), with conductances of 10 pS, 20 pS and 30 pS (12%, 25% and 37%) lower than the highest conductance state (*H*, 81 pS). The traces for +40 mV and −40 mV differ only in the frequency of substate switching. The conductance noise increased at high negative potential up to an amplitude of 1 pA at −l00 mV.

Nonlinear Dependence of Conductance on Electrolyte Concentration

Investigating the influence of the electrolyte concentration, we found that the single-channel conductance of TolC decreased as the ion concentration was lowered. Fig. 4*A* shows representative traces of single-channel measurements at ±60 mV at different KCl concentrations, pH 7.5. Above l00 mM KCl the conductivity measured at negative potentials was always higher, while below 100 mM it was lower than that measured at positive potentials. The noise at negative potentials increased as the ion concentration was reduced, reaching its maximum at 100 mM, while at positive voltage the noise level remained constantly low and substate switching was readily resolved (Fig. 4A).

Neither the frequency of substate switching nor substate lifetime was influenced by ion concentration. From 3 M to 200 mM the conductance decreased modestly as the voltage was applied over the range −120 mV and +120 mV (Fig. 4*B*). At lower ion concentrations this behavior was only observed when the potential was positive, while at negative potentials a conductance minimum was observed around −60 mV. These measurements show that there is no linear dependence between the single-channel conductance and the ion concentration. This was confirmed when the voltage was held at +60 mV or −60 mV. The conductance in each case reached a plateau at high salt concentrations (Fig. 4*C*).

pH-Dependence of the Single-Channel Conductance

To investigate the influence of the pH on TolC conductance we repeated the measurements made in Fig. 3*A* at different pH values. After a single TolC trimer had inserted into the membrane, the pH was lowered by addition of citrate. An example of the traces, from pH 4.3, is shown in Fig. 5, and the conductances from the entire pH-series are plotted against applied voltage in Fig. 6*A*. Several effects were evident:

(i) The single-channel conductance decreased at low voltages, from around 85 pS at pH 7.5 to below 20 pS at pH 3.7. Fig. 6*B* summarizes the pH dependence of the single-channel conductance at −20 mV. To obtain the *pK* of the apparent closing the conductance values (*G*) were fitted using a combination of the Henderson Hasselbalch equation

$$pH = pK + \log \frac{\alpha}{1-\alpha} \tag{1}$$

and the equation

$$G = G_{\text{low}} + (G_{\text{high}} - G_{\text{low}}) \cdot \alpha, \tag{2}$$

where G_{low} and G_{high} represent the single-channel conductance at very low and very high pH, and α is the acid dissociation rate. The resulting equation

$$G = G_{\text{low}} + (G_{\text{high}} - G_{\text{low}}) \cdot \frac{10^{pH-pK}}{1 + 10^{pH-pK}} \tag{3}$$

was used to calculate the *pK*. The *pK* of the apparent closing is 4.5, derived from G_{low} = 9.5 pS and G_{high} = 83.7 pS.

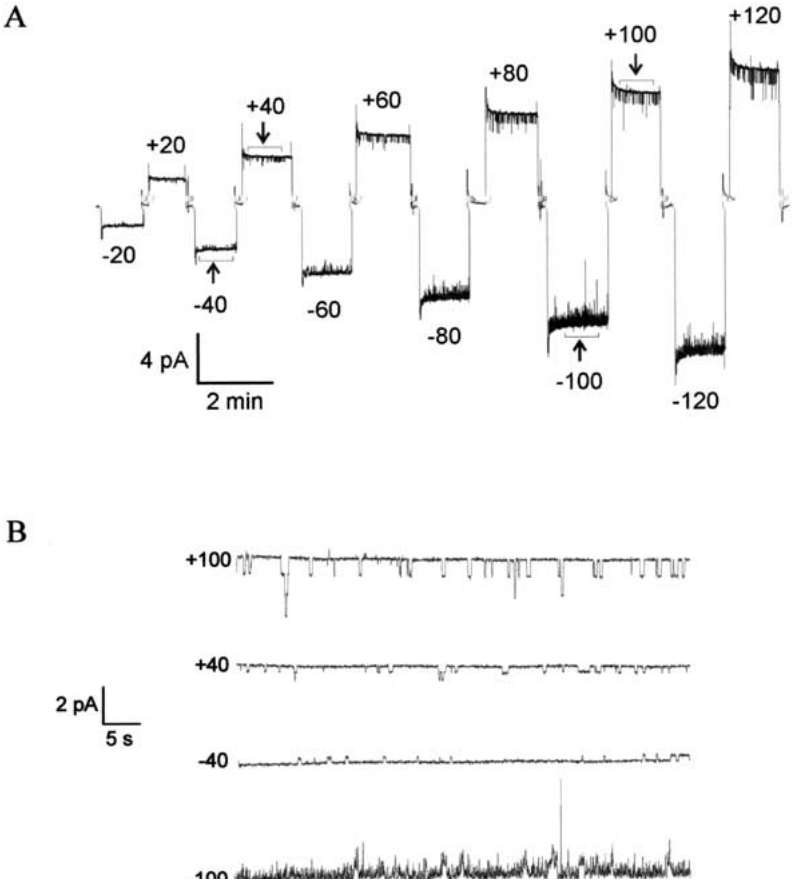

Fig. 3. Dependence of single-channel conductance on the size of the membrane potential (mV as shown). (*A*) Current through a single TolC molecule recorded at different membrane potentials. TolC was added to a final concentration of 1–5 pg/ml. Other parameters were as in Fig. 2. (*B*) Higher time resolution of traces indicated by the arrows.

(ii) The decrease in conductance depended on polarity. When the potential was positive, there was a major decrease in conductance between pH 6.5 and pH 5.2, but when the potential was negative, there was a continuous decrease in conductivity from pH 7.5 to 3.7. At high negative potential, the influence of acidic pH weakened, the conductance increased strongly with potential and nearly reached the conductance seen at neutrality. When the potential was positive a major increase in conductance was only observed at high positive potentials and pH values below 4.3.

(iii) The influence of the pH on the relative magnitude of the substates was dependent on the polarity. Fig. 7*A* shows the behavior of a single TolC at different pH, at either +80 mV (upper traces) or −80 mV (lower traces). TolC was most often in the highest conductance state (*H*), but switches into as many as three substates (*S1*, *S2*, *S3*) were observed under all the conditions. In Fig. 7*B* the conductance states at different pH are summarized. The differences between the four conductance states changed with pH. Under neutral conditions they were of equal size (*see* also Fig. 3*B*), but when the pH was lowered the difference between *H* and *S1* was bigger than that between *S1* and *S2*. The rarely observed switch from *S2* into *S3* was even smaller, as was evident at pH 5.2 for positive potential and at pH 4.1 for negative potentials.

(iv) At low pH and high negative potential, further substates of relatively low and variable conductance were rarely seen. The Fig. 5 inset shows several switches into substates of between 13 pS and 27 pS, corresponding to 20% and 40% of the highest conductance state *H* (67 pS). Another switch into a very noisy substate of 10 pS occurred when the voltage was −100 mV. In the experiment depicted the voltage was returned to zero, but if the voltage was kept constant the noisy substate persisted (*not shown*). At low pH and high positive potential there were short-lived spikes of variable conductance (Fig. 5).

Ion Selectivity of TolC

Measurements of ion selectivity were performed in a multi-channel experiment. TolC was added to one side of the membrane and the zero-current potential was measured after establishing a 10-fold gradient across the membrane (30 mM and 300 mM KCl, pH 7.5). When the higher concentration was on the TolC-proximal side the zero-current potential was 47.1 ± 2.4 mV (mean of 9 measurements), positive on the side of the lower concentration. Changing the

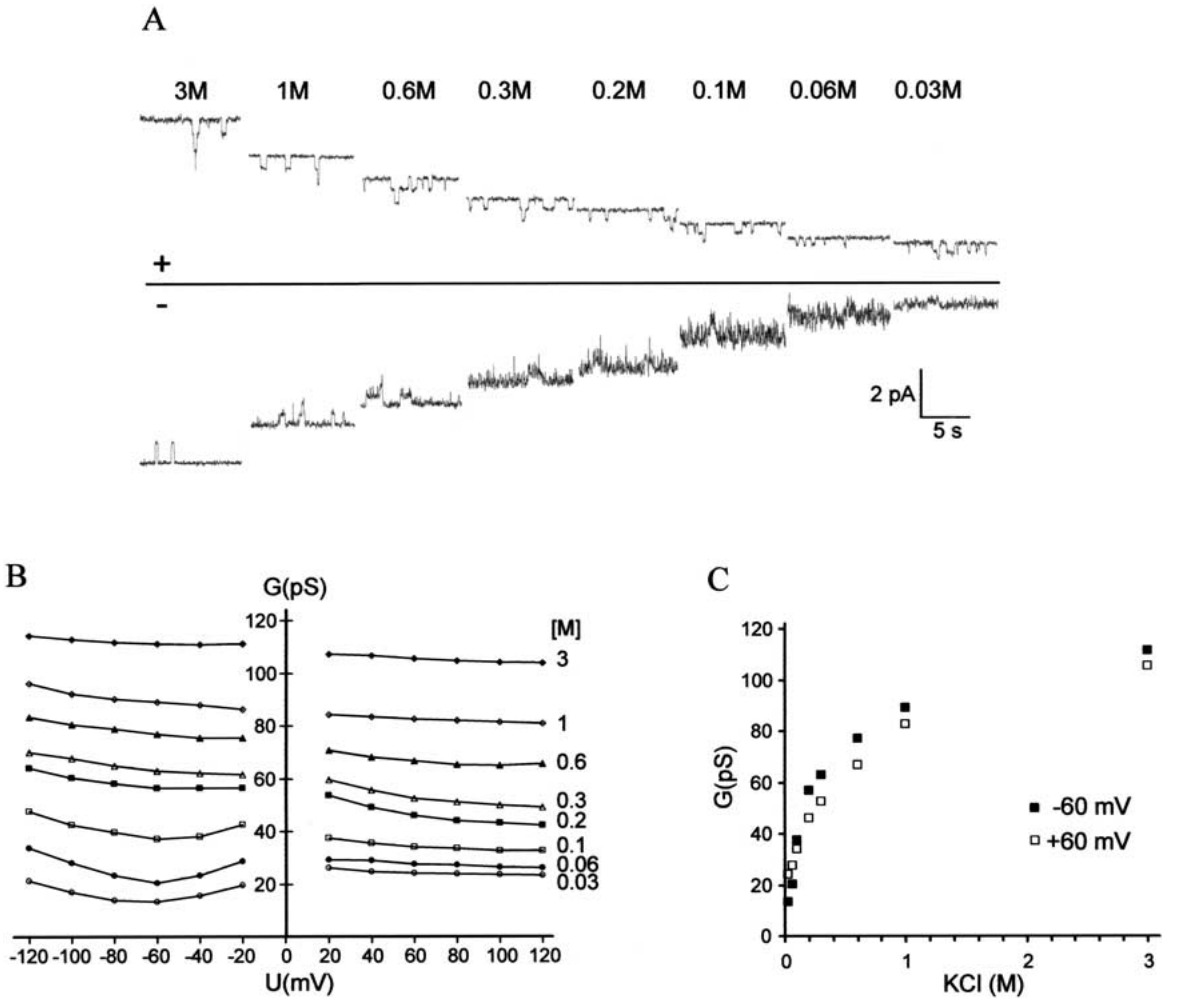

Fig. 4. Dependence of TolC single-channel conductance on electrolyte concentration at pH 7.5. (*A*) Representative traces of a single channel at the molar electrolyte concentrations (M) indicated. The applied potential was either +60 mV (upper traces) or −60 mV (lower). (*B*) Summary of the effect of electrolyte concentration on the conductance. (*C*) Concentration dependence of the conductance measured at +60 mV and −60 mV.

orientation of the gradient (i.e., to lower concentration on the TolC-proximal side) did not affect the zero-current potential. In this case it was 47.4 ± 3.2 mV (7 measurements). Because the potential becomes positive on the side with the lower electrolyte concentration, the channel-tunnel is selective for cations. The Goldman-Hodgkin-Katz equation allows calculation of the relative cation/anion permeability (P_{cation}/P_{anion}). The value for TolC is 16.5, meaning it has a 16.5-fold higher permeability for potassium ions than for chloride anions.

Discussion

The TolC structure is unlike that of any other known protein. The analysis of its behavior in membranes is an essential prerequisite to detailed study, e.g., following mutation. Purified TolC reconstituted into planar lipid bilayers showed asymmetric electrophysiological behavior, consistent with its structure. Because of the hydrophilic exterior of the tunnel, TolC is expected to insert always with the channel domain first into the lipid bilayer. Such structurally dictated asymmetric insertion into artificial membranes has been described, e.g., by the mushroom-shaped *Staphylococcus aureus* α-hemolysin (Song et al., 1996). The rate of TolC insertion was unaffected by the polarity, indicating that membrane potential is not required, in contrast for example to the insertion of colicins E1 and B and the lantibiotic nisin (Merill & Cramer, 1990; Pressler et al., 1986; Sahl, Kordel & Benz, 1987). Pores formed by the TolC channels are very stable and do not show the voltage-dependent gating.

TolC was highly cation-selective, in agreement with single-channel conductance measurements made in different electrolytes (Benz, Maier & Gentschev,

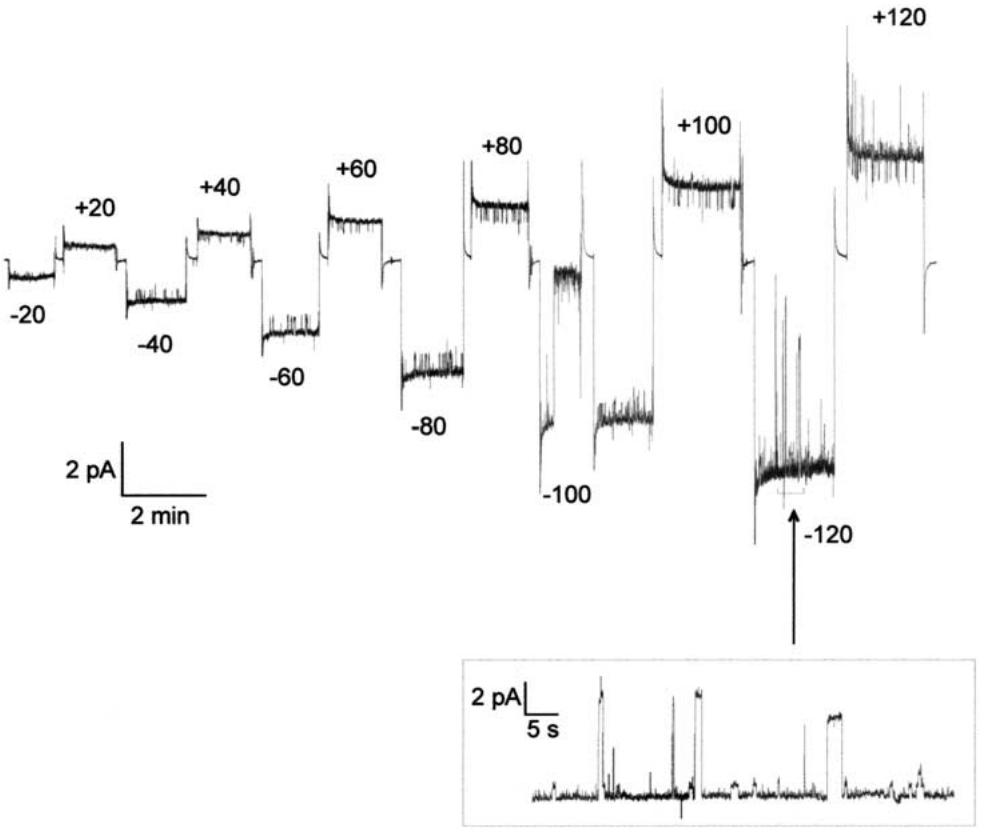

Fig. 5. Dependence of single-channel conductance on the membrane potential at pH 4.3. The inset shows a higher time resolution of the trace indicated by the arrow.

1993). The *E. coli* porins OmpF, OmpC and LamB are similarly selective (Benz, Schmid & Hancock, 1985; Benz, Schmid & Vos-Scheperkeuter, 1987). Their selectivity is strongly influenced by interior amino-acid residues, mostly located in or opposite to the inward-folded loop that constricts the porin channel (Hancock et al., 1986; Saint et al., 1996). TolC has no constriction point in the membrane-spanning channel or in the body of the tunnel, which both have a fairly constant inner diameter of 35Å (Koronakis et al., 2000; Andersen et al., 2000). Only the tapered helices of the tunnel determine constriction at the periplasmic entrance, and this can be assumed to be the principal determinant of conductance. Fig. 8 shows a cross section of the entrance, which is lined by two aspartates of each monomer (Asp371 and Asp374), facing inwards at two successive helical turns. The distance between Asp374 residues is 6.1 Å, between Asp371 residues 6.7 Å. They establish a highly electronegative area, which might determine cation selectivity. Measurements of the zero-current potential suggested a relative cation/anion permeability (P_{cation}/P_{anion}) of 16.5, which means that the current through the channel-tunnel is determined principally by cation flux. Reproducibly, TolC conductance was larger when the TolC-proximal side was negative. A reason for this could be that TolC may act like a concentrating 'funnel' if cations flow in the direction of the periplasmic entrance, but not if they flow in the opposite direction.

Large channels like the *E. coli* general diffusion pores show a linear dependence of single-channel conductance on ion concentration (Benz, Janko & Läuger, 1979), while other pore-forming proteins like the hemolysin of *Proteus vulgaris* or the cell wall porin of *Nocardia asteroides* show a nonlinear dependence (Benz, Hardie & Hughes, 1994; Riess et al., 1998). TolC dependence was also nonlinear. At low salt concentration, negative charges at the periplasmic entrance, especially Asp371 and Asp374, could accumulate cations so that the concentration here may differ from that of the bulk phase. At high concentration, TolC dependence resembled a saturation curve, which may reflect limitation of the ion flux by the small periplasmic opening. At negative potential, TolC noise increased as ion concentration was reduced (Fig. 4*A*). This might be explained by the ion concentration affecting the Debye-length of charged molecules, which reflects the decay of the potential in relation to the distance from the charge. The higher the ion concentration the smaller the Debye-length

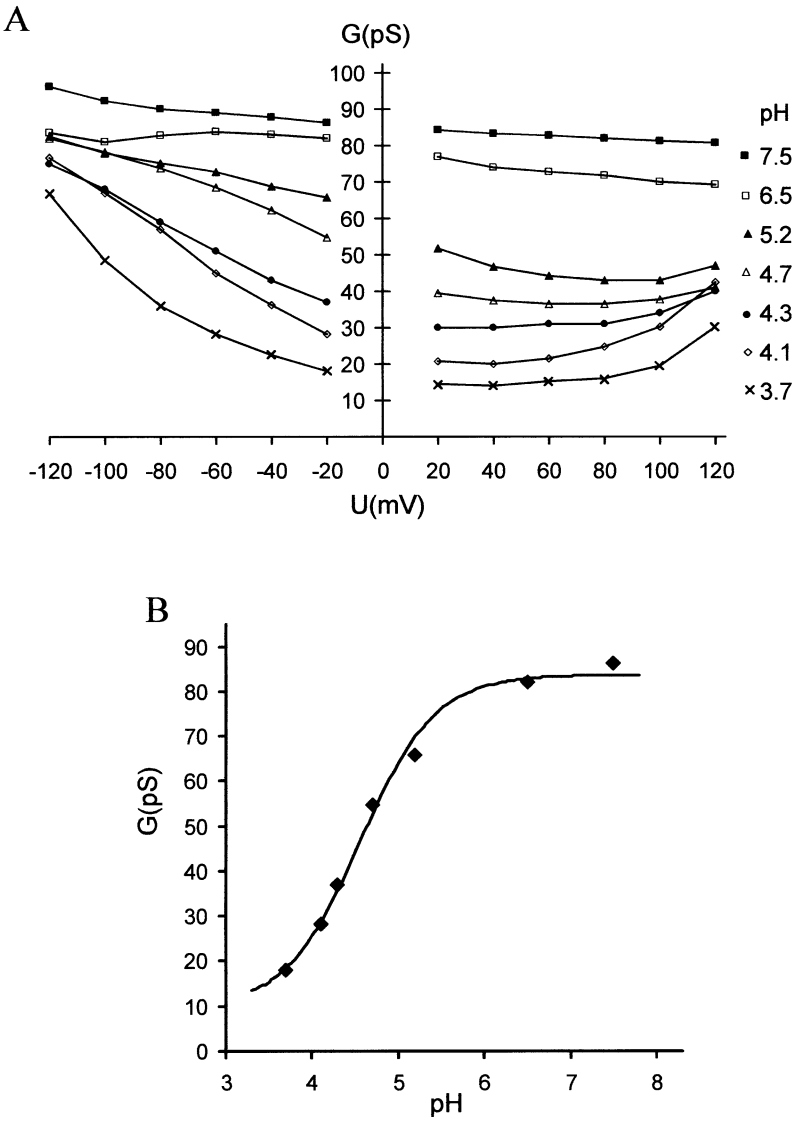

Fig. 6. pH dependence of the single-channel conductance. (*A*) The pH range of 3.7–7.5 was established using HEPES and citrate with negative (*left*) or positive (*right*) potential applied to the TolC-proximal side. (*B*) pH dependence of the conductance at −20 mV. The fit curve was derived as described in the text.

(e.g., in aqueous solution at 25°C, the Debye-length decreases from 30 Å at 10 mM, to 3 Å at 1 M), which means that at low ion concentration the area influenced by a charge would be much larger than at high concentrations, when the charge would be shielded by the ions. It also means that charges would be more sensitive to the applied potential at lower ion concentrations, which might explain why comparable TolC noise is observed at −60 mV, 300 mM KCl, and −80 mV, 1 M KCl (*see* Fig. 2 and Fig. 4*A*). It is possible that the origin of the noise can be the proposed conformational mobility of the extracellular loops (Koronakis et al., 2000), which contain the positively charged residues Lys265 and Arg267. At high negative potential the loops can be pulled into the channel leading to a labile constriction. A similar increase in noise has been observed where unstable extracellular loops lead to flickering at the channel entrance of engineered variants of maltoporin (Andersen et al., 1999).

TolC conductance decreased at low pH indicating a reduction of the diameter of the tunnel entrance. The calculated *pK* was 4.5, which would be compatible with involvement of a glutamate (*pK* 4.3–4.5) at the entrance. The only candidate is Glu359 of helix H7, which forms a hydrogen bond with Gln136 of H3 (*see* Fig. 8). Interruption of this interaction could allow movement of the inner helix pair H7/H8. This would constrict the entrance and reduce the single-channel conductance. The biggest reduction was observed at small membrane potentials (±20 mV). At higher negative potential and with the concomitant higher cation flux towards the periplasmic entrance, the constriction of the entrance appeared to be reversed, perhaps by outwards movement of the helices. At −120 mV the conductance nearly reached levels seen at neutrality. With positive potential a strong increase in conductance was only seen above 100 mV when the pH was below 4.3. This behavior might be

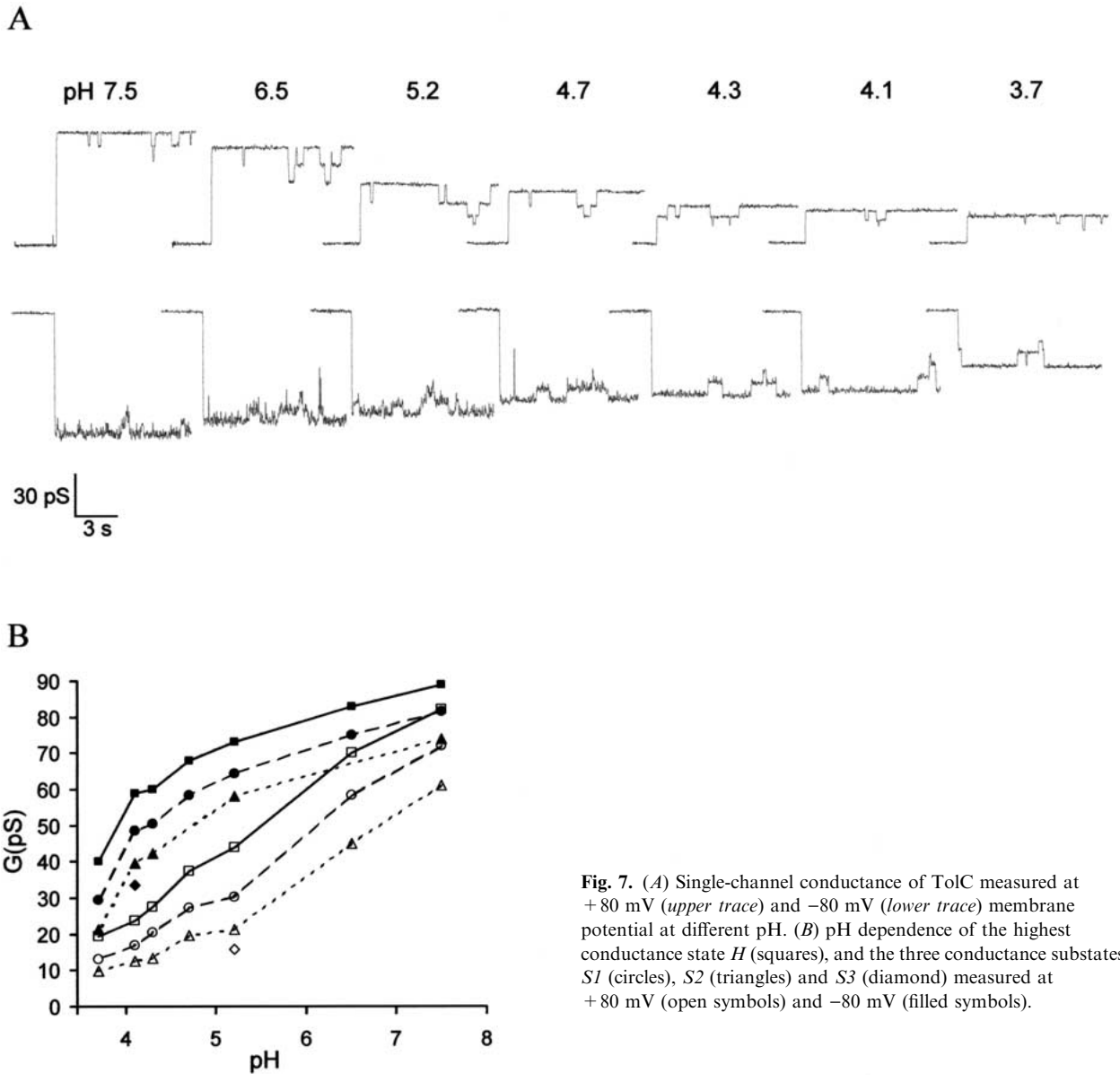

Fig. 7. (*A*) Single-channel conductance of TolC measured at +80 mV (*upper trace*) and −80 mV (*lower trace*) membrane potential at different pH. (*B*) pH dependence of the highest conductance state *H* (squares), and the three conductance substates *S1* (circles), *S2* (triangles) and *S3* (diamond) measured at +80 mV (open symbols) and −80 mV (filled symbols).

explained by protonation of Asp371 and Asp374 (*pK* 3.9–4.0) at lower pH, reducing the negative charges at the tunnel entrance and weakening cation selectivity, especially as at positive potential the anion flux towards the entrance could also encourage the proposed funnel effect. These aspartate residues could also be involved in determining the reduced single-channel conductance at low pH. Under neutral conditions their negative charges could repel the helix pairs from each other, while reducing the charge by protonation at low pH would diminish this effect and could lead to an inward movement of the helix pairs.

At all pH values, there were frequent switches into substates. Although these switches were not the same size at positive and negative potentials, it is reasonable to assume that they have the same origin, conformational changes at or near the tunnel entrance. Three substates were evident. In a previous study without pH-dependence assays this observation led to the erroneous conclusion that TolC comprises three individual channels characteristic of porins (Benz et al., 1993). We show that the magnitude of the TolC switches were equal at neutral pH, but at lower pH the switch into *S1* was the largest, with the switch from *S1* into *S2* and *S2* into *S3* progressively smaller. These data highlight the unipore structure of TolC (comparable analyses of the raffinose-uptake porin RafY have shown that in a porin the switch into the first of three substates is the smallest and the switch from the second to the third is the biggest; Andersen et al., 1998). Constriction of the tunnel entrance caused by the inward movement of the helix

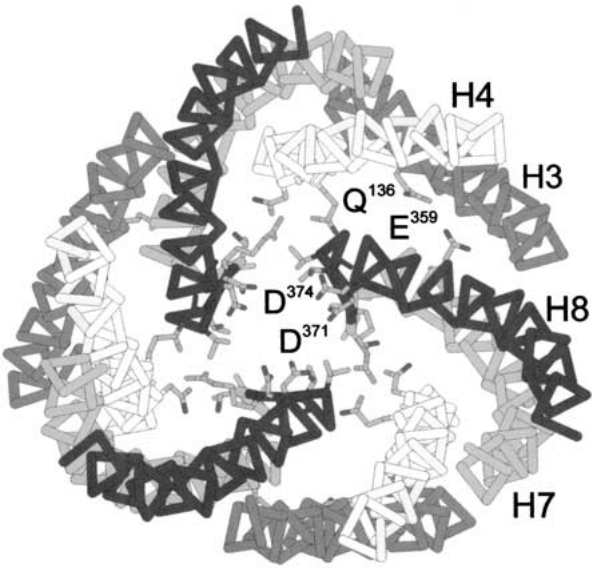

Fig. 8. The TolC entrance. View down the TolC tunnel towards the periplasmic opening. Helices are shaded gray (*H3*), white (*H4*), light gray (*H7*), and dark gray (*H8*). Only side chains of residues facing into the tunnel lumen near the entrance are shown except Glu359 and Glnl36, which are discussed in the text. The figure was made using RASMOL.

pairs *H7*/*H8* at lower pH could explain why the switches between the three TolC substates are not equal, as successive conformational changes in each of the three monomers would have a decreasing impact on the constriction of the single pore (the size of the switch into *S1* decreased when *H* was <40 pS, and this could reflect the critical diameter of the tunnel entrance). At low pH and negative potential there was sporadic switching to substates with very low conductance. The cause is unclear but perhaps the proposed iris-like entrance becomes unstable, with one of the three H7/H8 helix pairs moving further inward and reducing the opening still more. The short-lived increases in conductivity at high positive potential and low pH might also reflect instability, in this case of a labile open state that collapses immediately back to the stable closed state.

The negatively charged amino acids at the periplasmic entrance are highly conserved in the large TolC family (Andersen et al., 2000), suggesting that most or all of the channel-tunnels are also cation-selective. In addition to precluding entry by negatively charged noxious substances, these charges could be involved in the export and efflux functions, e.g., threading peptide chains into the tunnel or facilitating movement of drugs towards the outer membrane channel. In none of our experiments, in which high voltage, high electrolyte concentration and low pH were applied, did we observe the fully open state of the channel-tunnel that would reflect its biological function during export. Even urea added to a final concentration of 3 M failed to open TolC (*not shown*). Clearly, the folding at the periplasmic entrance is extremely stable until triggered to open by contact with the substrate-engaged inner membrane complexes. The characterization of TolC presented in this paper will facilitate the unravelling of this opening mechanism.

We thank Eva Koronakis and Jeyanthy Eswaran for critically reading the manuscript. Our work is supported by a Medical Research Council Programme grant (VK & CH) and an EMBO Fellowship (CA).

References

Andersen, C., Bachmeyer, C., Täuber, H., Benz, R., Wang, J., Michel, V., Newton, S.M., Hofhung. M., Charbit, A. 1999. In vivo and in vitro studies of major surface loop deletion mutants of the *Escherichia coli* K-12 maltoporin: contribution to maltose and maltooligosaccharide transport and binding. *Mol. Microbiol.* **32:**851–867

Andersen, C., Hughes, C., Koronakis, V. 2000. Chunnel vision: Export and efflux through bacterial channel-tunnels. *EMBO Rep.* **1:**313–318

Andersen, C., Krones, D., Ulmke, C., Schmid, K., Benz, R. 1998. The porin RafY encoded by the raffinose plasmid pRSD2 of *Escherichia coli* forms a general diffusion pore and not a carbohydrate-specific porin. *Eur. J. Biochem.* **254:**679–684

Benz, R., Hardie, K.R., Hughes, C. 1994. Pore formation in artificial membranes by the secreted hemolysins of *Proteus vulgaris* and *Morganella morganii*. *Eur. J. Biochem.* **220:**339–347

Benz, R., Janko, K., Boos, W., Läuger, P. 1978. Formation of large, ion-permeable membrane channels by the matrix protein (porin) *of Escherichia coli*. *Biochim. Biophys. Acta* **511:**305–319

Benz, R., Janko, K., Läuger, P. 1979. Ionic selectivity of pores formed by the matrix protein (porin) of *Escherichia coli*. *Biochim. Biophys. Acta* **551:**238–247

Benz, R., Maier, E., Gentschev, I. 1993. TolC of *Escherichia coli* functions as an outer membrane channel. *Zentralbl. Bakteriol.* **278:**187–196

Benz, R., Schmid, A., Hancock, R.E. 1985. Ion selectivity of gram-negative bacterial porins. *J. Bacteriol.* **162:**722–727

Benz, R., Schmid, A., Vos-Scheperkeuter, G.H. 1987. Mechanism of sugar transport through the sugar-specific LamB channel of *Escherichia coli* outer membrane. *J. Membrane Biol.* **100:**21–29

Cowan, S.W., Schirmer, T., Rummel, G., Steiert, M., Ghosh, R., Pauptit, R.A., Jansonius, J.N., Rosenbusch, J.P. 1992. Crystal structures explain functional properties of two *E. coli* porins. *Nature* **358:**727–733

Forst, D., Welte, W., Wacker. T., Diederichs. K. 1998. Structure of the sucrose-specific porin ScrY from *Salmonella typhimurium* and its complex with sucrose. *Nat. Struct. Biol.* **5:**37–46

Fralick, J.A. 1996. Evidence that TolC is required for functioning of the Mar/AcrAB efflux pump *of Escherichia coli*. *J. Bacteriol.* **178:**5803–5805

Hancock, R.E., Schmidt, A., Bauer, K., Benz, R. 1986. Role of lysines in ion selectivity of bacterial outer membrane porins. *Biochim. Biophys. Acta* **860:**263–267

Koronakis, V., Li, J., Koronakis, E., Stauffer, K. 1997. Structure of TolC, the outer membrane component of the bacterial type I efflux system, derived from two-dimensional crystals. *Mol. Microbiol.* **23:**617–626

Koronakis, V., Sharff, A., Koronakis, E., Luisi, B., Hughes, C. 2000. Crystal structure of the bacterial membrane protein TolC central to multidrug efflux and protein export. *Nature* **405:**914–919

Merrill, A.R., Cramer, W.A. 1990. Identification of a voltage-responsive segment of the potential-gated colicin E1 ion channel. *Biochemistry* **29:**8529–8534

Pressler, U., Braun, V., Wittmann-Liebold, B., Benz, R. 1986. Structural and functional properties of colicin B. *J. Biol. Chem.* **261:**2654–2659

Riess, F.G., Lichtinger, T., Cseh, R., Yassin, A.F., Schaal, K.P., Benz, R. 1998. The cell wall porin of *Nocardia farcinica:* biochemical identification of the channel-forming protein and biophysical characterization of the channel properties. *Mol. Microbiol.* **29:**139–150

Sahl, H.G., Kordel, M., Benz, R. 1987. Voltage-dependent depolarization of bacterial membranes and artificial lipid bilayers by the peptide antibiotic nisin. *Arch. Microbiol.* **149:**120–124

Saint, N., Lou, K.L., Widmer, C., Luckey, M., Schirmer, T., Rosenbusch, J.P. 1996. Structural and functional characterization of OmpF porin mutants selected for larger pore size. II. Functional characterization. *J. Biol. Chem.* **271:**20676–20680

Song, L., Hobaugh, M.R., Shustak, C., Cheley, S., Bayley, H., Gouaux, J.E. 1996. Structure of staphylococcal alpha-hemolysin, a heptameric transmembrane pore. *Science* **274:**1859–1866

Thanabalu, T., Koronakis, E., Hughes, C., Koronakis, V. 1998. Substrate-induced assembly of a contiguous channel for protein export from *E.coli*: reversible bridging of an inner-membrane translocase to an outer membrane exit pore. *EMBO J.* **17:**6487–6496

Wandersman, C., Delepelaire, P. 1990. TolC, an *Escherichia coli* outer membrane protein required for hemolysin secretion. *Proc. Natl. Acad. Sci.* **87:**4776–4780

Zgurskaya, H.I., Nikaido, H. 2000. Multidrug resistance mechanisms: drug efflux across two membranes. *Mol. Microbiol.* **37:**219–225